OPERATING POINT AND STRIPPING EXTRACTION CALCULATIONS FOR CYCLONE 10/5

Wang Liangming (王良明)

(Institute of Nuclear Science and Technology, Sichuan University, Chengdu 610064, China)

S.Zaremba

(Ion Beam Applications s.a., Chemin du Cyclotron 2, B-1348 Louvain-la-Neuve, Belgium)

(Received January 1991)

ABSTRACT

By using the magnetic field map, equilibrium orbit, operating point of ν_r and ν_z and beam trajectories after stripper for Cyclone 10/5 have been calculated. The positions of two strippers and two targets have been determined. The numerical simulation is consistent with experimental tests.

Keywords: Isochronous cyclotron Operating point Revolution frequency Betatron oscillation frequency Equilibrium orbit Stripping extraction

The Cyclone 10/5 is a fixed field, fixed frequency, isochronous cyclotron designed for the acceleration of H^- ions up to a maximum energy of 10 MeV and D^- ions up to 5 MeV. The negative ions are extracted and converted into positive ions by stripping in a thin carbon foil. It is specifically designed for clinical P.E.T (Positron Emission Tomography) centers.

The pole plates are designed in a four-sector symmetry geometry and the pole diameter is 80 cm. The air gap is 3 cm between poles and 65 cm for valley. The magnetic field of Cyclone 10/5 was realized according to theoretical calculations by program Poisson. The azimuthal lengths of the sector are calculated and adjusted to reach the required isochronous main field value for different radii with a radial step of half centimeter. The proposed magnetic field is isochronous for protons. The positions of two stripping foils and two targets were theoretically calculated.

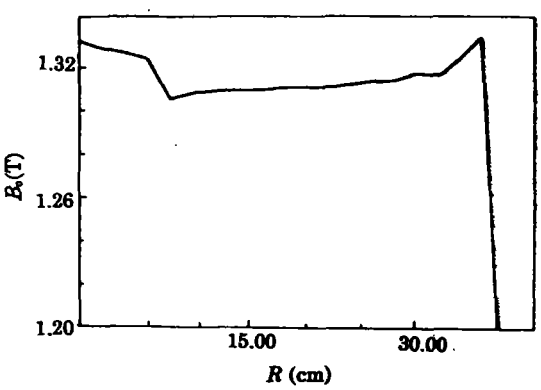

Fig.1 The isochronous magnetic field of C 10/5

The realized magnetic field in the median plane of the cyclotron has been precisely measured with an azimuthal step of 2° and a radial step of 2 cm until radius of 46 cm is reached. A prolongations of the magnetic field for a greater radius have been achieved until the fringing field equals

zero. All data above have been used to creat a map of the magnetic field. Fig.1

Table 1

The average magnetic field from realized magnetic field map and the theoretical magnetic field

Radius (cm)	B_{theory} (10^{-1}T)	B_{real} (10^{-1}T)	Radius (cm)	B_{theory} (10^{-1}T)	B_{real} (10^{-1}T)
0	11.2422	13.3189	30	13.1247	13.1879
2	11.2947	13.2840	32	13.0834	13.1786
4	11.9975	13.2728	34	13.0313	13.2435
6	13.8265	13.2447	36	12.7839	13.3550
8	13.5781	13.0573	38	10.6315	11.5494
10	12.8355	13.0884	40	6.1690	6.9026
12	12.6659	13.0979	42	3.9758	4.4768
14	12.5708	13.1048	44	2.8936	3.2517
16	12.5112	13.1035	46	2.2462	2.5137
18	12.4698	13.1098	48	1.7902	1.2070
20	12.4379	13.1172	50	1.4313	0.2279
22	13.2327	13.1172	52		0.0133
24	13.2082	13.1330	54		0.0002
26	13.1833	13.1568	56		0.0000
28	13.1562	13.1565	58		0.0000

Table 2

The first–, second– and third–harmonic field perturbations from Fourier series

Radius (cm)	A_1 (10^{-1}T)	A_2 (10^{-1}T)	A_3 (10^{-1}T)	B_1 (10^{-1}T)	B_2 (10^{-1}T)	B_3 (10^{-1}T)
0	–0.0026	–0.0014	–0.0007	–0.0027	0.0003	0.0005
2	0.0013	–0.0014	–0.0006	–0.0006	0.0003	0.0001
4	0.0011	0.0000	0.0012	–0.0053	0.0049	–0.0086
6	–0.0041	0.0041	0.0031	0.0109	0.0124	–0.0266
8	–0.0059	0.0047	0.0013	0.0146	0.0111	–0.0301
10	–0.0077	0.0017	–0.0003	0.0127	0.0098	–0.0295
12	–0.0070	–0.0010	–0.0023	0.0125	0.0081	–0.0270
14	–0.0076	–0.0034	–0.0036	0.0114	0.0078	–0.0247
16	–0.0075	–0.0056	–0.0041	0.0105	0.0077	–0.0236
18	–0.0073	–0.0076	–0.0048	0.0101	0.0075	–0.0222
20	–0.0076	–0.0094	–0.0052	0.0089	0.0071	–0.0209
22	–0.0075	–0.0103	–0.0052	0.0093	0.0081	–0.0200
24	–0.0076	–0.0012	–0.0056	0.0103	0.0088	0.0185
26	–0.0077	–0.0119	–0.0060	0.0103	0.0093	–0.0175
28	–0.0073	–0.0123	–0.0064	0.0100	0.0091	–0.0167
30	–0.0058	–0.0122	–0.0065	0.0104	0.0092	–0.0165
32	–0.0042	–0.0116	–0.0069	0.0104	0.0085	–0.0162
34	–0.0036	–0.0108	–0.0073	0.0109	0.0081	–0.0159
36	–0.0024	–0.0103	–0.0085	0.0141	0.0047	–0.0146
38	0.0133	–0.0015	–0.0139	0.0444	–0.0370	0.0016
40	0.0115	0.0056	–0.0071	0.0334	–0.0282	0.0037
42	0.0064	0.0076	–0.0024	0.0212	–0.0111	0.0006
44	0.0032	0.0086	–0.0012	0.0175	–0.0048	0.0000
46	0.0030	0.0095	–0.0009	0.0191	–0.0024	–0.0003
48	0.0000	0.0000	0.0000	0.0000	0.0000	0.0000

presents the average isochronous magnetic field *vs* cyclotron radius.

The Fourier transform of the magnetic field has been obtained until radius 74 cm. The maximum harmonic number of Fourier series (multiplied by 4 internally in program) is 20. The analytical Fourier series shows that the imperfections of magnetic field are acceptable. The average magnetic field from Fourier series is different from proposed theoretical magnetic field due to several reasons, for example, the vacuum causing changes of gap between magnet poles, the tolerances from mechanical processing and the theoretical permeability of the iron. The differences are mainly as follows: the realized average magnetic field of the central region is higher than theoretical values, but equal approximately in middle region and lower in prolongation field, radially, see table 1.

The analytical Fourier series was used to find revolution frequency of particles and to certify an isochronism in Cyclone 10/5 for protons. The Fourier series was used because the hard edge approximation method was used for the prolongation fringing field of magnetic field radially with problems in a numerical integration of differential equation system at the connection places between hill and valley, see table 2.

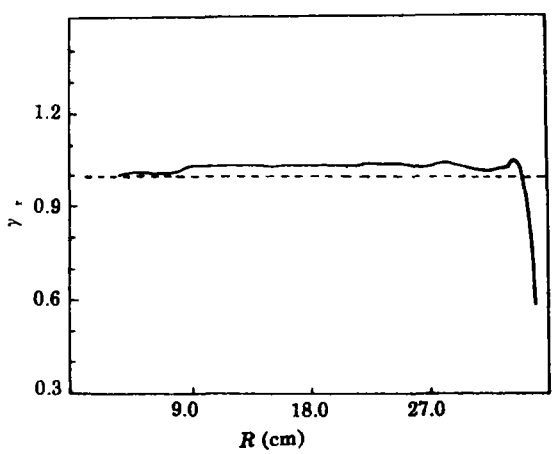

Fig.2 The radial betatron oscillation frequencies for C 10/5

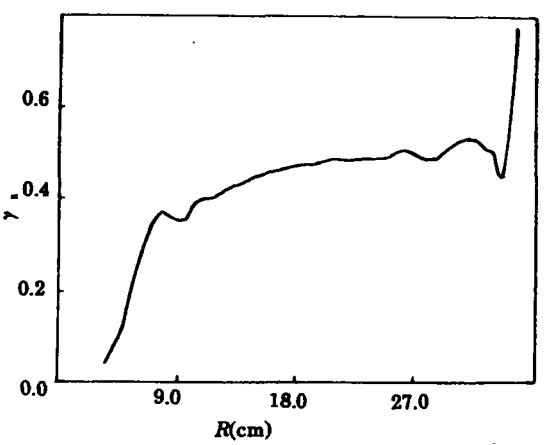

Fig.3 The axial betatron oscillation frequencies for C 10/5

Calculations show that the realized magnetic field yields simultaneously the necessary radial and axial stability of the orbit motion. A voltage gain per turn of 60 keV is obtained with a peak rf potential of 30 kV. The revolution frequencies of particles are resonant from 20.229 to 20.260 MHz and frequency chosen for calculations is 20.240 MHz.

The betatron oscillation frequencies ν_r and ν_z have been calculated with numerical orbit integration. It shows that ν_r approximately equals 1 and drops below 1 in the extraction region, ν_z grows from 0.04 to relatively high value of 0.542. It is clearly seen that three resonances are crossed during proton acceleration, $\nu_r = 2\nu_z$

difference resonance (Walkinshaw resonance) at 7.5 MeV, 9.1 MeV and 9.2 MeV,

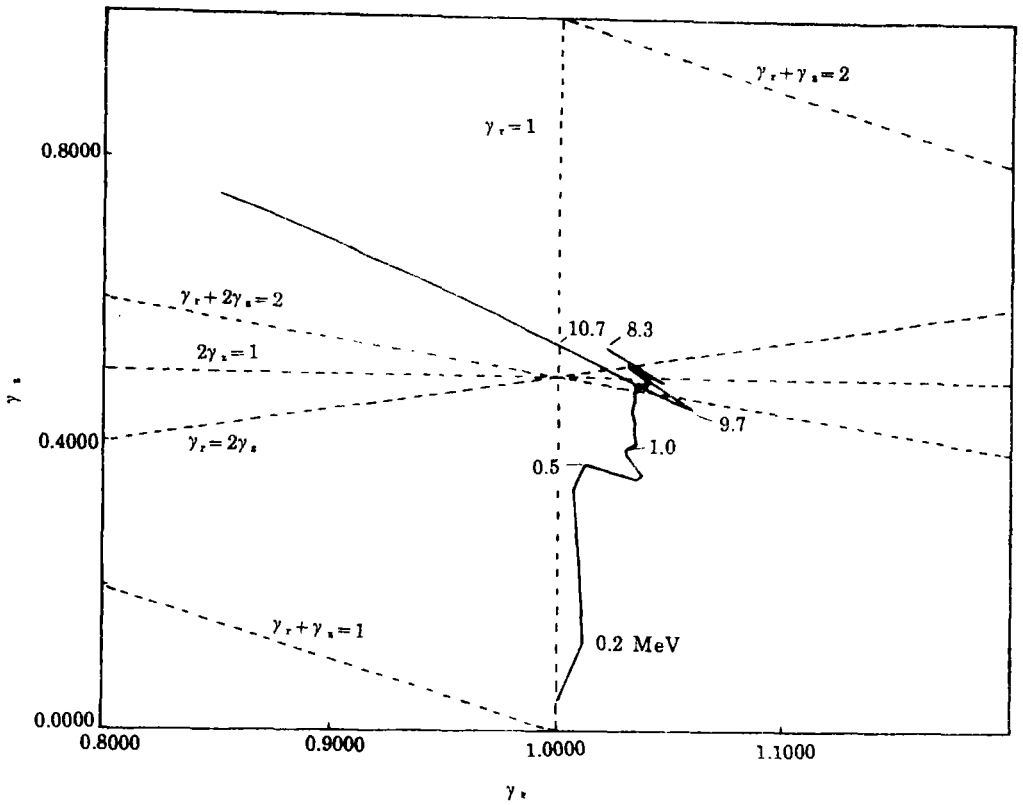

Fig.4 The operating point of C10/5 (ν_r—ν_z)

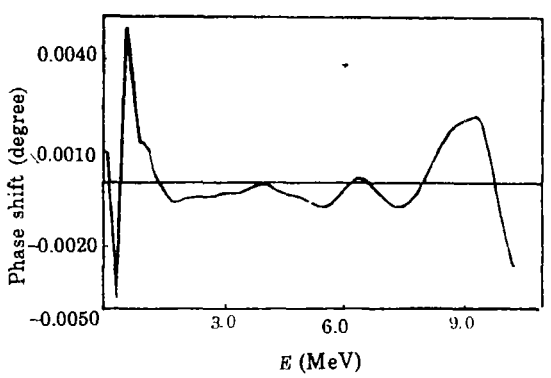

Fig.5 The phase shift (turn/turn) of C 10/5

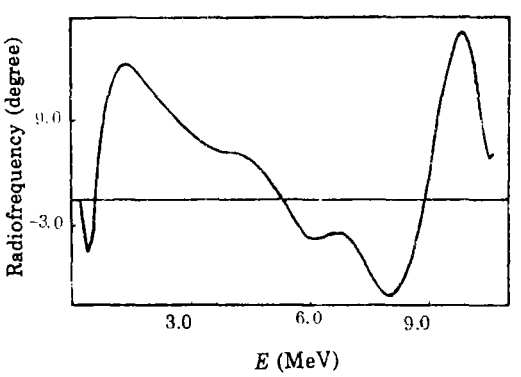

Fig.6 The integrated phase shift (2 harmonic) of C 10/5

$2\nu_z=1$ imperfection resonance at 5.4 MeV, 6.4 MeV, 7.2 MeV and 9.3 MeV, sum resonance $\nu_r+2\nu_z=2$ at 3.4 MeV, 9.6 MeV and 9.9 MeV.

Fig.2–3 present the values of ν_r and ν_z as a function of the average orbit radius. Fig.4 presents the operating point of ν_r and ν_z. The rf accelerating system consists of two dees assembled in two opposite valleys. Two dees are connected at the center.

Second harmonic mode acceleration is used and an azimuthal length of dee is about 30°. This azimuthal length corresponds to 60° radio frequency phase shift between two successive accelerating gaps for proton. The calculated rf integrated phase shift is from −10.98° to +19.93° with respect to desired reference frequency 20.240 MHz. Fig.5 presents the phase shift from turn to turn and figure 6 the integrated phase shift.

Also numerically equilibrium orbit was calculated for required H^- with kinetic energy 10 MeV. Particles for 10 MeV H^- were traced along the equilibrium orbit and an action of a carbon foil was simulated by a change of the particle charge state. Proton trajectories after stripper were calculated until radius of 60 cm is reached.

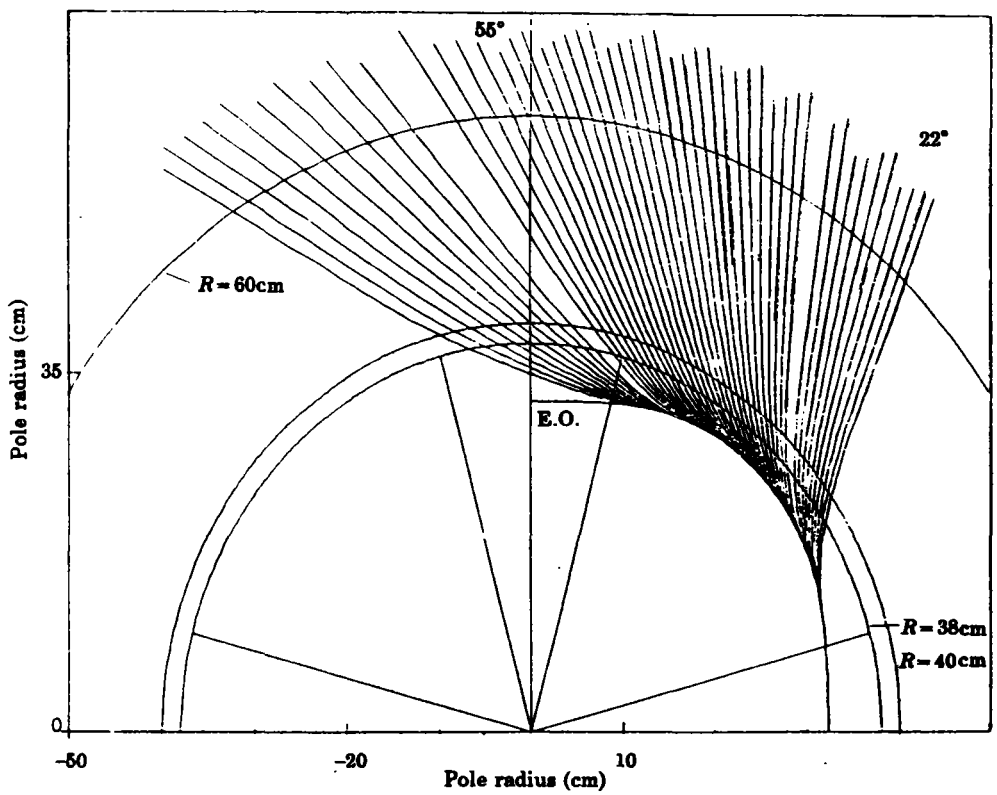

Fig.7 The equilibrium orbit and trajectory after stripper of C 10/5

Fig.7 presents proton trajectories for different stripper positions. Stripper positions have been changed every 1 degree of azimuth started from 20° to 70° and the start point is measured from the symmetry axis of the magnet valley in a counter-clockwise direction. A choise of the stripper and target position has to take the geometrical dimensions of stripper and target mechanical assemblies into account. Two strippers and two targets do not obstruct each other at following positions which can be considered as one possible solution. All angles are measured with respect to the symmetry axis of the valley of the magnetic field and distances are measured with respect to the cyclotron center. Both targets are placed 600 mm from the cyclotron

center. The azimuthal target position as a function of the azimuthal position of the stripper is presented in figure 8. The first stripper is at azimuth 22° with a distance 339.13 mm, the second stripper at azimuth 55° with a distance 351.6 mm, the first target at azimuth 49.49°, and the second target at azimuth 90.30°.

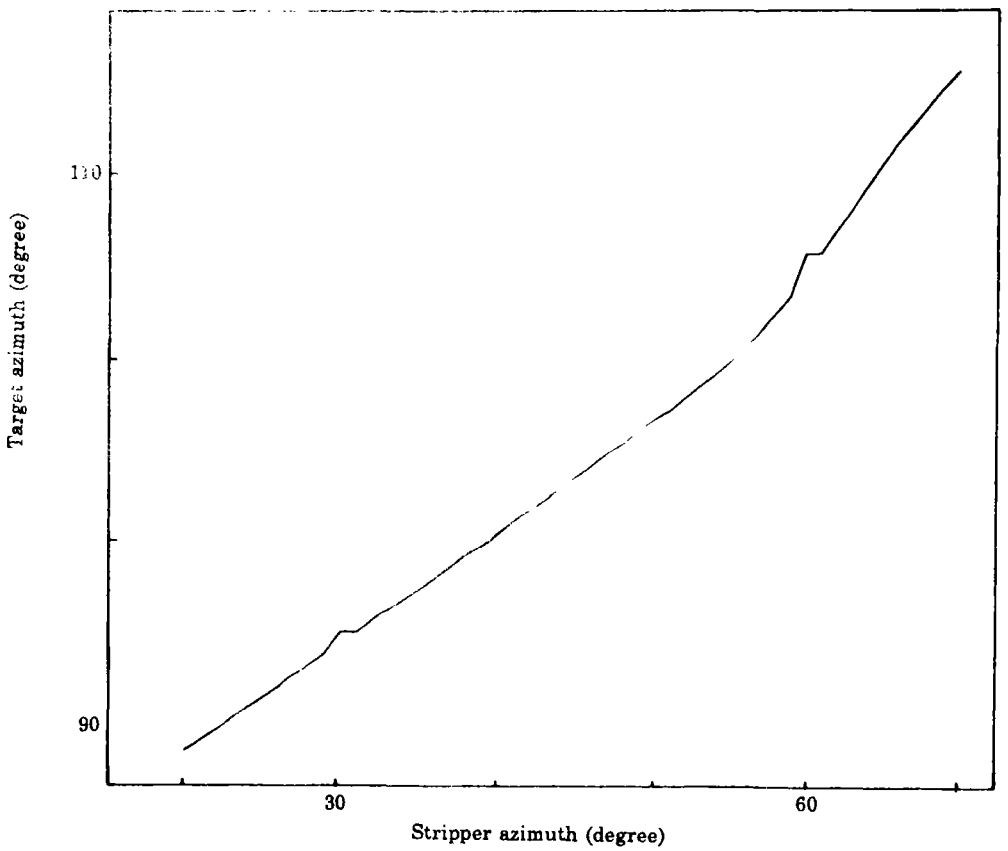

Fig.8 Target azimuth vs stripper azimuth (target radius 60 cm)

CONCLUSIONS

The first beam test results proved that the theoretical calculations of the magnetic field and the calculations of the extraction system were correct. The maximum difference of the beam position on the target between numerical simulation and experimental tests was less than 10 mm.

ACKNOWLEDGEMENTS

One (Wang) of the authors is grateful to I.B.A. for providing a good condition of making research work.